AGU PUBLICATIONS

Geophysical Research Letters

RESEARCH LETTER
10.1002/2015GL067327

Key Points:
- Geomorphological prediction of dust sources compared with long-term dust loading from MODIS
- Predicted rank importance of geomorphology for dust emissions confirmed by satellite record
- Geomorphological dynamics can predict dust emissions and should be included in global dust models

Correspondence to:
M. C. Baddock,
m.c.baddock@lboro.ac.uk

Citation:
Baddock, M. C., P. Ginoux, J. E. Bullard, and T. E. Gill (2016), Do MODIS-defined dust sources have a geomorphological signature?, *Geophys. Res. Lett.*, *43*, 2606–2613, doi:10.1002/2015GL067327.

Received 7 DEC 2015
Accepted 2 MAR 2016
Accepted article online 9 MAR 2016
Published online 18 MAR 2016

Do MODIS-defined dust sources have a geomorphological signature?

Matthew C. Baddock[1], Paul Ginoux[2], Joanna E. Bullard[1], and Thomas E. Gill[3,4]

[1]Department of Geography, Loughborough University, Loughborough, UK, [2]NOAA Geophysical Fluid Dynamics Laboratory, Princeton, New Jersey, USA, [3]Environmental Science and Engineering Program, University of Texas at El Paso, El Paso, Texas, USA, [4]Department of Geological Sciences, University of Texas at El Paso, El Paso, Texas, USA

Abstract The preferential dust source (PDS) scheme enables large-scale mapping of geomorphology in terms of importance for dust emissions but has not been independently tested other than at local scales. We examine the PDS qualitative conceptual model of surface emissivity alongside a quantitative measurement of dust loading from Moderate Resolution Imaging Spectroradiometer (MODIS) Deep Blue Collection 6 for the Chihuahuan Desert. The predicted ranked importance of each geomorphic type for dust emissions is compared with the actual ranked importance as determined from the satellite-derived dust loading. For this region, the predicted variability and magnitude of dust emissions from most surface types present coincides with the observed characteristics demonstrating the significance of geomorphological controls on emission. The exception is for areas of low magnitude but persistent emissions such as alluvial surfaces where PDS overpredicts dustiness. As PDS is a good predictor of emissions and incorporates surface dynamics it could improve models of future dust emissions.

1. Introduction

Plumes of mineral dust are emitted into the atmosphere from source regions with specific geomorphological properties [*Reheis and Kihl*, 1995; *Schepanski et al*., 2007; *Bullard et al*., 2008; *Wang et al*., 2008; *Crouvi et al*., 2012; *Parajuli et al*., 2014]. In addition to influencing emission processes, composition, and fluxes, land surface properties are a key control on the nature of mineral aerosol [*Shao et al*., 2011]. Specifically, physical and chemical properties of dust aerosols that determine the strength of interactions between dust and radiation, as well as with cloud microphysics and biogeochemistry, are modulated by the nature of sediments in source areas [e.g., *Mahowald et al*., 2009; *Woodage and Woodward*, 2014]. Human activities also significantly affect erodibility, and thus dust emission [*Gill*, 1996; *Ginoux et al*., 2010, 2012; *Lee et al*., 2012].

Satellite remote sensing has been instrumental in establishing the global distribution of dust sources [*Prospero et al*., 2002; *Washington et al*., 2003; *Ginoux et al*., 2012]. The methodology consists of attributing source areas to locations associated with the most frequent dust detection, independently of land surface characteristics. At this global scale, the major terrestrial dust source regions are identified as internally draining basins in semiarid and arid regions; however, it is acknowledged that most basins include a mosaic of different land surface types with different propensities to emit dust. Several studies have examined the relative contributions of landforms within major dust-emitting basins, e.g., Lake Eyre Basin, Australia [*Bullard et al*., 2008], southern Africa [*Vickery et al*., 2013], the eastern Great Basin [*Hahnenberger and Nicoll*, 2014] and Southern High Plains, USA [*Lee et al*., 2012], and North American Chihuahuan Desert [*Baddock et al*., 2011]. Such studies, alongside field investigations [e.g., *McTainsh et al*., 1999; *Sweeney et al*., 2011], have demonstrated the variable contributions from different land surface types, highlighting the importance of this variability for understanding the dynamics of dust source regions as a whole. To reflect the variable dust emissivity of different land surfaces, a geomorphology-based classification known as the Preferential Dust Source scheme was developed [*Bullard et al*., 2011]. The preferential dust source (PDS) comprises a suite of geomorphological classes defined by their differing potentials to emit dust. To date, however, there has been little independent examination of whether surfaces predicted to be important for dust emissions actually coincide spatially with areas identified as dust sources using satellite remote sensing [*Parajuli et al*., 2014].

To address this, our paper analyzes the geomorphic properties associated with dust sources in the Chihuahuan Desert by comparing a long-term remote sensing aerosol data set with the PDS geomorphology-based potential dust emission scheme. We use an updated version of *Ginoux et al.'s* [2012] MODIS Deep Blue inventory, with

its advantages of being recent, global, and offering a decade of highly spatially resolved daily data. Determining whether land surface types that are predicted to be persistent dust sources are actually identified as such in the long-term MODIS dust loading record provides a first regional- and decadal-scale validation of the approach. The land surface mapping and aerosol data sets we use are independent, with no overlap between the data used to create them. Investigating the relationship between the two data sets tests a qualitative conceptual model of surface emissivity against a quantitative measurement of dust loading.

2. Methods and Study Region

2.1. PDS Scheme

The PDS scheme provides an improved method of representing the land surface amenable to large-scale dust modeling efforts. PDS suggests, via sedimentology, soil properties and the key limitations to emissions associated with different types of geomorphology (e.g., sediment supply and availability [*Kocurek and Lancaster*, 1999]), that certain land surfaces are more persistent and favored dust sources than others [*Bullard et al*., 2011]. The scheme holds that ephemeral and dry lakes, and unarmored, unincised alluvial surfaces of high relief have highest potential to be persistent dust emission sources. Sources of moderate potential include unarmored low relief alluvial surfaces, sand sheet, and some aeolian dune systems. Stony surfaces (e.g., desert pavement), alluvial surfaces with armoring, and bedrock or duricrusts are all unlikely to be dust sources.

The relationship of the PDS scheme to observed dust activity has been assessed with reference to satellite-derived dust source point maps [*Bullard et al*., 2011]. While successful in pinpointing locations of active emission to a high degree of spatial resolution, point source mapping offers a limited representation of emission magnitude from different surfaces. Furthermore, the limitations of the approach preclude a complete sampling of dust source activity [*Lee et al*., 2009, 2012]. Examining the relationship between the PDS classification and a broad-scale, aerosol product-based mapping of dust loading offers an improved assessment of the scheme's ability to represent persistent emission sources [*Parajuli et al*., 2014]. With its reliable, multiyear data set of dust observations, the latest version of MODIS Deep Blue provides the means to validate PDS.

2.2. Study Area and PDS Mapping

The PDS classification scheme has been successfully applied to several major dust-bearing regions, with its full conceptual development detailed by *Bullard et al*. [2011]. Here we investigate the Chihuahuan Desert (CD), as defined by *Schmidt* [1979]. Using landform and soils data sets from Mexico and the U.S., a map of land unit polygons was created for the CD. Through high-resolution satellite imagery, geological, and soil maps, and fieldwork, each polygon within the CD area was attributed to a PDS class. Of 17 possible PDS surface classes, 11 are present within the CD. For the CD mapping process and data sources, see *Baddock et al*. [2011].

The CD is one of the most active dust sources in North America [*Prospero et al*., 2002]. Dust is raised primarily by synoptic-scale Pacific cold fronts and deepening cyclones to the northeast during the cold (dry) season [*Rivera Rivera et al*., 2009, 2010]. These systems produce large areas of strong southwesterly winds frequently capable of entraining sediment for many hours. Mesoscale, convective events (haboobs), triggered by thunderstorm outflows or dry microbursts, drive dust emission in the warm season [*Novlan et al*., 2007] and are limited in space and time compared to cold-season dust outbreaks.

2.3. Dust Source Detection Using MODIS Deep Blue

Using methods for regular 0.1° gridding of Level 2 MODIS Deep Blue (M-DB2) aerosol products [*Ginoux et al*., 2010, 2012], a global map of Collection 6 (C6) M-DB2 data has been created. Improvements in surface reflectivity and algorithm retrieval mean that C6 MODIS DB aerosol products, both absolute aerosol optical depth (AOD) and its spectral variation, have changed compared to C5.1 [*Hsu et al*., 2013; *Sayer et al*., 2013]. Consequently, the Angstrom exponent, a proxy of aerosol size distribution, calculated as the logarithm of the ratio of AOD at two wavelengths divided by the logarithm of the inverse ratio of these wavelengths, was employed in C6. Previous studies demonstrated that persistent dust sources can be identified from the frequency of observation (FoO) of elevated dust signals [*Prospero et al*., 2002]. Here we first extract the Dust Optical Depth (DOD) from the spectral AOD and single-scattering albedo retrieved by *Hsu et al*. [2013], by imposing a maximum Angstrom exponent of 0.3 (to separate dust from other fine particles) and single-scattering albedo <1 because dust is slightly absorbing. The annual mean FoO of DOD >0.2 (2003–2014) is used as our base to detect dust events [*Ginoux et al*., 2012].

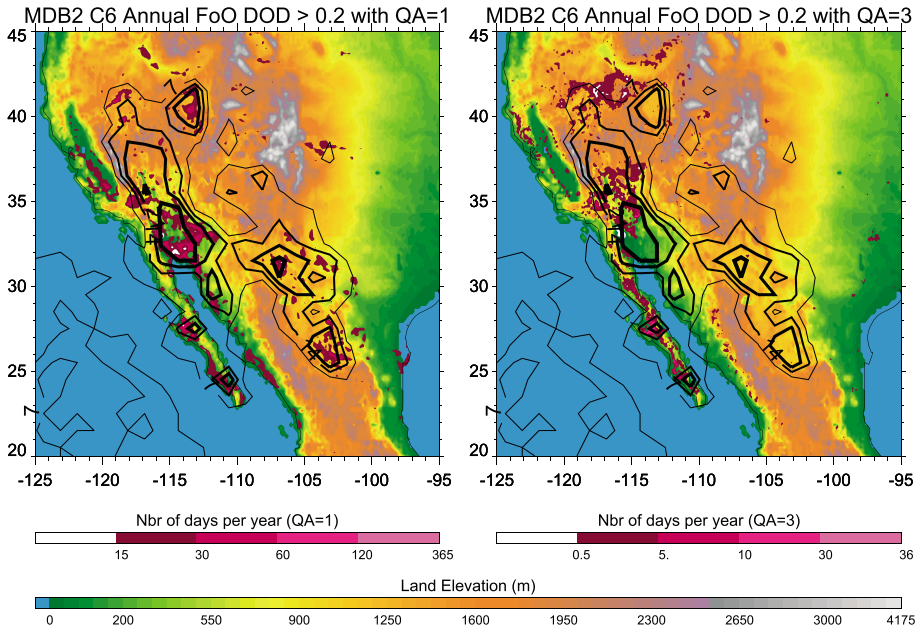

Figure 1. Mean annual FoO of DOD > 0.2 at (left) QA = 1 and (right) QA = 3 for M-DB2 over southwestern North America, overlain with TOMS AI FoO contours from *Prospero et al.* [2002].

Contrary to the suggestion by *Hsu et al.* [2013] of using aerosol products flagged as very good quality (QA = 3), we use the lowest quality flag (QA = 1). The reason is that high- and medium-quality flags are based on a maximum standard deviation of 0.18 and 0.15 over 10 × 10 pixels of 1 km. Over dust sources, the standard deviation is much larger, and retrieved aerosol products are flagged poorly. Figure 1 shows annual mean FoO of DOD > 0.2 over North America for QA = 1 and QA = 3, FoO from Total Ozone Mapping Spectrometer (TOMS) Nimbus 7 Aerosol Index (AI, version 7) > 0.7, and topography (Plate 2, *Prospero et al.* [2002]). While all hot spots of TOMS AI coincide with M-DB2 FoO for QA = 1, this is not the case for QA = 3. Furthermore, FoO values for QA = 1 are fivefold greater. We therefore recommend using QA = 1 for dust source detection.

Since DOD values will be elevated to some extent throughout dust-bearing regions, for specific source identification, a threshold can be applied to DOD to determine areas of persistently high dust loading, and therefore emission. From DOD observed for sources at a global scale, *Ginoux et al.* [2012] presented a range of (C5.1) DOD thresholds at 0.25, 0.5, and 1, applicable to different regions. In optimizing for source identification in the CD and C6 DOD, we apply a DOD threshold of >0.75 to highlight sources. Interpreting FoO at this threshold increases confidence that areas defined spatially by high FoO are locations of persistent dust emission, rather than ambient dust or dust in transport (e.g., land surfaces lying under the most common dust pathways). DOD > 0.75 also eliminates most areas with diffuse dust and surfaces not expected to emit dust (e.g., open water).

3. Results

3.1. Spatial Distribution of Aerosol Loading

Figure 2a shows the long-term mean distribution of FoO for DOD > 0.75 ($FoO_{D0.75}$) in the CD. Across the region, FoO is spatially variable, with the main regions of elevated FoO located north of 30°N and south of 28°N. The maximum $FoO_{D0.75}$ in these regions is >10% of days for the 12 year period (thus, DOD > 0.75 for > ~440 days). *Gillette* [1999] identified "hot spots" as localized, persistent areas of intense dust production within an overall landscape which generally does not emit dust. The DOD threshold of 0.75 isolates the most intense dust sources in the CD. Four large hot spots where $FoO_{D0.75}$ > 5% emerge as key locations (Figure 2a).

Hot spot 1 is the White Sands region of New Mexico (center 106.25°W, 33°N), with approximately 2500 km^2 characterized by long-term $FoO_{D0.75}$ > 1%, and a maximum FoO five times this in localized places. Hot spot 2 is the Salt Basin of southwest Texas. Patches of $FoO_{D0.75}$ > 1% are found throughout this 3500 km^2 area. The maximum is a relatively constrained area of $FoO_{D0.75}$ > 5% observed in the east of the region. In northern

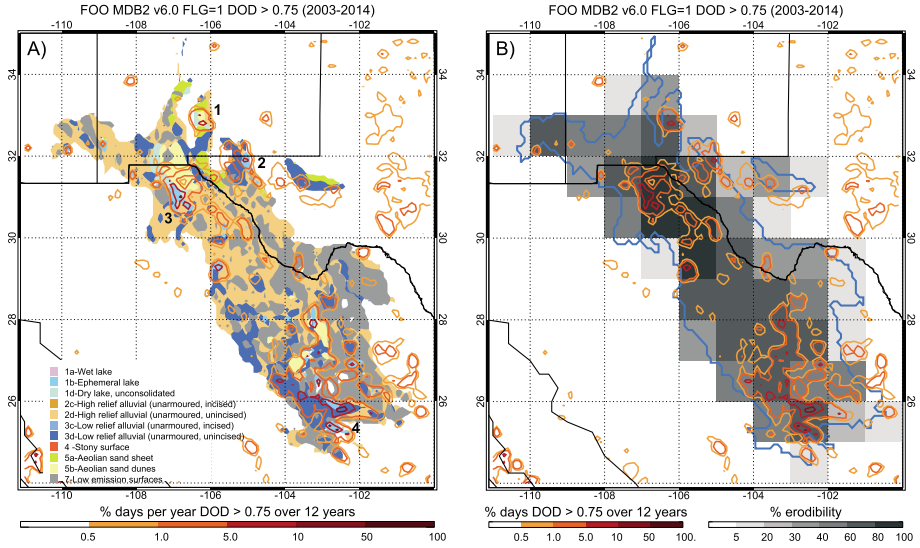

Figure 2. (a) Distribution of FoO (% days 2003–2014) for DOD > 0.75 over PDS classes for Chihuahuan Desert. (b) Same FoO distribution over 1 × 1° cells showing percentage of cell with geomorphology classed as medium- or high-emission potential by *Bullard et al.* [2011]. Numbers 1–4 indicate dust hot spots in text.

Chihuahua, Hot spot 3 is associated with the pluvial Lake Palomas complex. The coverage of $FoO_{D0.75} > 1\%$ is almost 7500 km^2 with FoO peaks up to 5% and 10% detected in the west and southwest of the region. Lying mostly below 28°N, Hot spot 4 is marked by a contiguous area of $FoO_{D0.75} > 1\%$, covering around 30,000 km^2 in the general Bolsón de Mapimí region of the southern CD. The distribution of regionally higher $FoO_{D0.75}$ (>5%) within the region is highly spotty, and the largest area of $FoO_{D0.75} > 10\%$ for the entire CD is detected in the southwest of this area. Aside from the four major locations, there are numerous relatively spatially discrete peaks in raised FoO associated with smaller valleys or basins.

3.2. Aerosol Loading by Surface Geomorphology

By examining the number of days on which DOD exceeded the 0.75 threshold for each PDS-classified cell (0.1°), the long-term average FoO for each PDS class was determined. The mean and variability of $FoO_{D0.75}$ for each land surface type is shown in Figure 3. In the CD, the highest mean FoOs are associated with three geomorphic surface classes: ephemeral lakes, dry unconsolidated lakes, and sand dunes. Considered as a whole, these three surface types exhibit a mean $FoO_{D0.75}$ of >1.35% for the study period, with ephemeral lakes showing the maximum of 2.45% days with DOD > 0.75. Observed variability in FoO is also highest for these three categories.

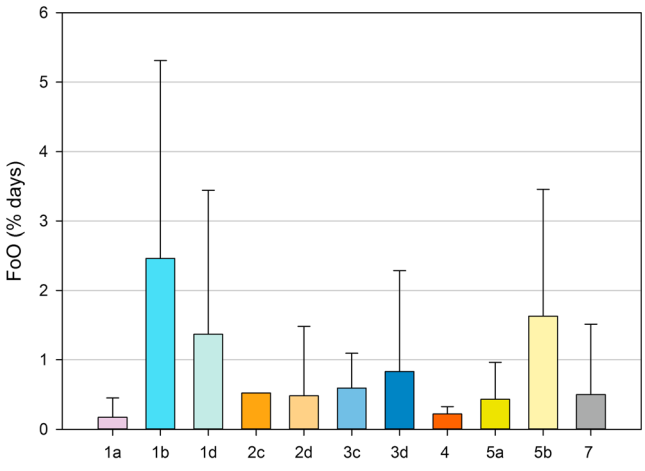

Figure 3. Mean FoO of DOD > 0.75 by PDS class in the Chihuahuan Desert (2003–2014), with standard deviations. Key for PDS classes in Figure 2a.

Relative to these persistently dusty surface types, unarmored, unincised low-relief alluvial surfaces (3d), which occupy most intermontane valleys of the CD, emerge as moderate sources, with $FoO_{D0.75}$ about one third of ephemeral lakes (0.83%). Sand sheet, stony surface, and incised, unarmored low-relief alluvial surfaces are all comparable to, or less than, the low-emission

surfaces category and emerge as the weakest emitters (FoO < 0.5%). The single most extensive geomorphology class in the CD (43% of area) is the unincised, unarmored high-relief alluvial (2d) category which represents the prevalent piedmont bajada slopes of the region. The mean $FoOD_{0.75}$ of this dominant surface type is similar to that of the low-emission surfaces (0.48% days). Wet lakes occupy <0.1% of the CD, and the existence of a (very low) FoO over these surfaces represents traces of dust transport over certain small water bodies.

4. Discussion and Conclusion

Figure 1 shows that the M-DB2 $FoO_{D0.75}$ distribution observed for the CD is very similar to *Prospero et al.'s* [2002] TOMS AI-based map of North American dust activity, with high activity to the north and south of a central area of relatively low activity. By identifying emission sources at higher spatial resolution, the M-DB2 approach adds significant detail to this broad pattern. As the M-DB2 data are independent of the PDS scheme, they can be used to determine whether those land surface types predicted to be persistent dust sources based on their geomorphology and sedimentology are actually associated with high mineral aerosol loadings in the long-term MODIS record.

Numerous field campaigns and analyses of satellite data have highlighted ephemeral and dry lakes as important dust sources [see *Bryant*, 2013]. Drawing upon these data and the sediments and sediment budget dynamics of these landforms, the PDS scheme predicts that they should be the most significant geomorphologies for dust emission [*Bullard et al*., 2011]. This prediction is confirmed here as ephemeral and dry lake classified areas in the CD are associated with the highest mean FoO in the long-term dust record (Figure 3). Conversely, the PDS scheme predicts that low-emission surfaces and stony ground will be the least significant dust source areas and that sand sheets have only medium- to low-emission potential. Again, this is confirmed as these geomorphologies in the CD are all associated with the lowest mean FoO (Figure 3).

In the PDS scheme, the importance of sand dunes for dust emissions ranges from low to high depending on factors such as dune type, composition, history, and location. Active quartz dune fields comprising well-sorted sand are typically weak dust sources [*Prospero et al*., 2002]. This describes the sandy Dunas de la Soledad area in the CD (103.75°W, 27°N), appearing as a nonpersistent source area (FoO < 0.5%) (Figure 2a). However, overall, sand dunes in the CD are generally associated with a high (but variable) mean FoO, comparable to unconsolidated dry lake surfaces. In previous studies, some of the highest dust emissions associated with dunes have been identified in areas where there is interplay between dunes and dry or ephemeral lake surfaces [*Lee et al*., 2009; *Baddock et al*., 2011] because the dunes provide saltating grains for sandblasting of and dust generation from the lacustrine deposits [*Cahill et al*., 1996]. Such a juxtaposition of landforms occurs at White Sands gypsum dune field within the CD [*White et al*., 2015] and also in the Lake Palomas basin where a sand sheet/nebkha dune field is adjacent to the lake sediments of El Barreal [*Rivera Rivera et al*., 2010]. Local FoO for these two dune-lake areas exceeds 5%. The variability of FoO associated with dune surfaces in the CD suggests that the wide range of predicted dust emissions from dunes in the PDS scheme is appropriate.

PDS also predicts that a significant type of alluvial surface for dust emissions will be those of high relief that are unarmoured and unincised (medium to high emissions) (2d). In the CD this geomorphology was associated with low mean FoO values (Figure 3), suggesting that the PDS scheme overpredicts dust emission from this land type. One possible explanation for this comes from *Floyd and Gill's* [2011] ecosystem-based analysis of CD aeolian fluxes which demonstrated that while playas produce the most dust per unit area, shrublands (broadly coincident with the "unarmored unincised high-relief alluvial" PDS class) likely produce more dust overall due to their extent. This land type covers ~140,000 km^2 (43%) of the CD, and while the amount of dust emission during individual events is relatively low (likely putting them below the DOD detection criterion), their larger spatial coverage and potential for high total aeolian mass flux may more than compensate for low emissivity. *Reheis and Kihl* [1995] similarly suggested that in North America's Great Basin and Mojave Deserts, alluvial regions produced a greater amount of dust overall than playas, despite lower emission rates, due to their greater areal extent.

This paper focuses on whether geomorphological units can be differentiated by their persistence as dust sources at the decadal scale. We do not consider annual variability of dust emissions in the CD, but insights into longer timescale controls on dust source dynamics can be gained. The PDS scheme states that the majority of dust sources with medium-to-high importance for emission are sediment supply limited [*Kocurek and Lancaster*, 1999] and prone to alternate between periods of intense dust activity fueled by a supply of sediment and periods of low dust emission due to a lack of sediment [*Gillette et al*., 1997; *Bullard et al*., 2008]. This "switching on-

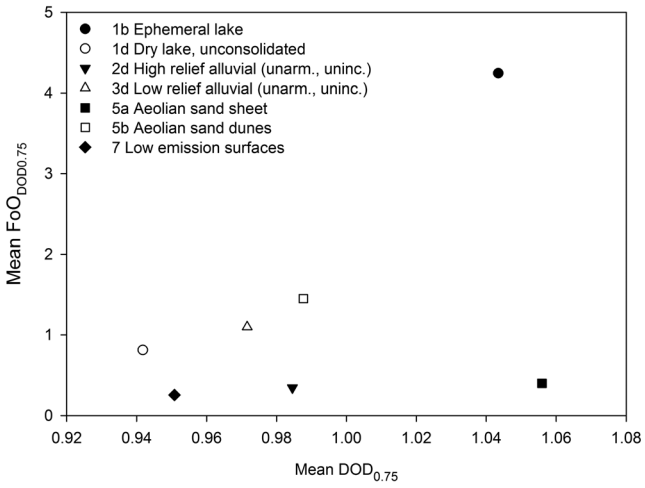

Figure 4. Average dust persistence (FoO) and magnitude (DOD) at DOD > 0.75 threshold, by geomorphology type. Mean values derived from 0.1° cells with >75% one geomorphology type.

switching off" dynamic results in highly variable dust emissions and, in the CD, is reflected in the pronounced variability of mean FoO for ephemeral lakes and both high- and low-relief unarmored alluvial surfaces (2d and 3d). However, variability in dust emissions can also be caused by fluctuations in transport capacity which can be regionally variable. For example, in the CD, two areas of low-relief, unincised, and unarmoured alluvial surface (the Salt Basin and parts of Bolsón de Mapimí) have been identified as emission hot spots while a large area with the same geomorphological characteristics centered on 105°W, 27°N has consistently low dust emissions. Although in a single regional dust event not all areas of similar geomorphology will emit simultaneously [e.g., *Gillette*, 1999; *Lee et al*., 2009], this spatial variability would be expected to average out in multiyear dust records, yet this is not the case for this CD area. One explanation is that under contemporary conditions, the weather systems responsible for the fastest winds in the CD do not frequently penetrate south of ~30°N [*Schmidt*, 1986], as also evidenced by climatic reconstructions from northern CD playas which suggest that strong westerlies and Pacific frontal systems lose dominance at latitudes south of Lake Palomas [*Scuderi et al*., 2010]. This lower transport capacity to the south, resulting in fewer exceedances of threshold velocity for entrainment, may help to explain the spatial variability in emission. In contrast, low-emission surfaces such as stony ground are typically sediment availability limited, a constraint on emission less subject to short-term change, as reflected in the low standard deviation of FoO for these surfaces (Figure 3).

Intrageomorphological variations in emission exemplify the challenges to incorporating emission heterogeneity in dust models [*Zender et al*., 2003; *Bullard*, 2010]. The small scale of dust hot spots shown here is an issue for dust models, because they cannot resolve features with scale lower than the model grid. As dust emission is initiated when surface winds reach a threshold for wind erosion, assumption of a mean threshold by grid cell will produce lower emission than by including subgrid variability with lower values over easily erodible surfaces. Figure 2b illustrates this by showing the proportion of gridded $1 \times 1°$ cells occupied by medium or highly erodible surfaces. Our results suggest that significant improvement in dust modeling may be achieved by considering the fraction of ephemeral and dry lakes and alluvial surfaces (due to their variability) within each grid cell using a high-resolution data set [cf. *Ginoux et al*., 2012] and applying a lower threshold of wind erosion on these surfaces.

The method used here also enables an examination of the relationship between not only persistence (mean FoO for DOD > 0.75) but also long-term magnitude (mean DOD > 0.75) of dust emissions from each surface class. This relationship is shown in Figure 4, but to isolate the different geomorphologies, only data from those 0.1° cells where a single surface type was dominant (>75% cell area) are included.

Of the 11 CD geomorphology classes, 7 had grid cells meeting the dominance criterion. Considering persistence and magnitude together, ephemeral lakes emerge as the most intense dust source. In comparison, dry unconsolidated lakes return a relatively low mean DOD and FoO, demonstrating the importance for emission magnitude of sediment supply provided by periodic inundations. While the mean DOD of sand sheets (5a) is comparable to ephemeral lakes, their overall intensity is strongly mitigated by depressed FoO, similar to low-emission surfaces (7). Dune-dominated cells (5b) exhibit a moderate emission magnitude in terms of mean DOD, which together with an elevated FoO, reinforces the suggestion that sedimentological conditions modulate dust generation from dune systems. Unincised, unarmored alluvial surfaces of both high (2d) and low relief (3d) occupy appreciable areas of the CD, and the absence of emission from large portions of these surfaces (Figure 2a) results in moderate overall magnitude. The low relief emerges as a more intense emitter, however, as its FoO is double that of the high-relief slopes.

In summary, applying a long-term distribution of dust loading from remote sensing to a land surface classification in the Chihuahuan Desert confirms fundamental linkages between geomorphology and dust emission. By examining the persistence of dust detection associated with specific geomorphology types, the preferential nature of emission from certain surfaces is quantified, the incorporation of which can improve representation of the land surface in dust models. To date, however, while detailed geomorphological mapping has been achieved for some regions, there is no standardized methodology or data set for global-scale coverage. In working toward such coverage, a promising recent development in machine learning for classifying dust source land surfaces has recently been demonstrated by *Lary et al*. [2016]. The intercomparison of aerosol loading and mapped emission potential in the CD offers a first-order validation of the PDS scheme, highlighting at a detailed spatial resolution the relative significance of different surface types including the dominance of ephemeral lakes. This study established long-term spatial agreement between land surface classes and dust emission, but time-averaged dust distributions overlook the geomorphological and meteorological dynamics which are key to explaining seasonal and annual emission patterns. Inherent to the PDS classification is the temporal pattern of dust emission associated with each geomorphology type (e.g., susceptibility to flooding and frequency of sediment supply), and having established the validity of the scheme spatially, the next step will be to explore how these temporal variations can be modeled.

Acknowledgments

Partially supported by a NOAA R2O NGGPS grant (P.G.) and NOAA cooperative agreements NA17AE1623 and NA17AE1625 (T.G.). The authors are grateful to Miguel Dominguez Acosta for discussions. MODIS C6 Deep Blue is available at the Level-1 and Atmosphere Archive and Distribution System (LAADS) Distributed Active Archive Center (https://ladsweb.nascom.nasa.gov). We thank Carlos Perez Garcia-Pando and an anonymous reviewer for comments.

References

Baddock, M. C., T. E. Gill, J. E. Bullard, M. Dominguez Acosta, and N. I. Rivera Rivera (2011), A geomorphic map of the Chihuahuan Desert, North America, based on potential dust emissions, *J. Maps*, *2011*, 249–259, doi:10.4113/jom.2011.1178.

Bryant, R. (2013), Recent advances in our understanding of dust source emission processes, *Prog. Phys. Geogr.*, *37*, 397–421, doi:10.1177/0309133313479391.

Bullard, J. (2010), Bridging the gap between field data and global models: Current strategies in aeolian research, *Earth Surf. Processes Landforms*, *35*, 496–499, doi:10.1002/esp.1958.

Bullard, J. E., S. P. Harrison, M. Baddock, N. A. Drake, T. E. Gill, G. H. McTainsh, and Y. Sun (2011), Preferential dust sources: A geomorphological classification designed for use in global dust-cycle models, *J. Geophys. Res.*, *116*, F04034, doi:10.1029/2011JF002061.

Bullard J., M. Baddock, G. McTainsh, and J. Leys (2008), Sub-basin scale dust source geomorphology detected using MODIS. *Geophys. Res. Lett.*, *35*, L15404, doi:10.1029/2008GL033928.

Cahill, T. A., T. E. Gill, J. E. Reid, E. A. Gearhart, and D. A. Gillette (1996), Saltating particles, playa crusts and dust aerosols from Owens (Dry) Lake, California, *Earth Surf. Processes Landforms*, *21*, 621–639.

Crouvi, O., K. Schepanski, R. Amit, A. R. Gillespie, and Y. Enzel (2012), Multiple dust sources in the Sahara Desert: The importance of sand dunes, *Geophys. Res. Lett.*, *39*, L13401, doi:10.1029/2012GL052145.

Floyd, K. W., and T. E. Gill (2011), The association of land cover with aeolian sediment production at Jornada Basin, New Mexico, USA, *Aeolian Res.*, *3*, 55–66, doi:10.1016/j.aeolia.2011.02.002.

Gill, T. E. (1996), Eolian sediments generated by anthropogenic disturbance of playas: Human impacts on the geomorphic system and geomorphic impacts on the human system, *Geomorphology*, *17*, 207–228, doi:10.1016/0169-555X(95)00104-D.

Gillette, D. A. (1999), A qualitative geophysical explanation for hot spot dust emitting source regions, *Contrib. Atmos. Phys.*, *72*, 67–77.

Gillette, D. A., D. W. Fryrear, T. E. Gill, T. Ley, T. A. Cahill, and E. A. Gearhart (1997), Relation of vertical flux of particles smaller than 10 μm to total aeolian horizontal mass flux at Owens lake, *J. Geophys. Res.*, *102*, 26,009–26,015, doi:10.1029/97JD02252.

Ginoux, P., D. Garbuzov, and N. C. Hsu (2010), Identification of anthropogenic and natural dust sources using Moderate Resolution Imaging Spectroradiometer (MODIS) Deep Blue level 2 data, *J. Geophys. Res.*, *115*, D05204, doi:10.1029/2009JD012398.

Ginoux, P., J. M. Prospero, T. E. Gill, N. C. Hsu, and M. Zhao (2012), Global-scale attribution of anthropogenic and natural dust sources and their emission rates based on MODIS Deep Blue aerosol products, *Rev. Geophys.*, *50*, RG3005, doi:10.1029/2012RG000388.

Hahnenberger, M., and K. Nicoll (2014), Geomorphic and land cover identification of dust sources in the eastern Great Basin of Utah, USA, *Geomorphology*, *204*, 657–672, doi:10.1016/j.geomorph.2013.09.013.

Hsu, N. C., M.-J. Jeon, C. Bettenhausen, A. M. Sayer, R. Hansell, C. S. Seftor, J. Huang, and S.-C. Tsay (2013), Enhanced Deep Blue aerosol retrieval algorithm: The second generation, *J. Geophys. Res. Atmos.*, *118*, 9296–9315, doi:10.1002/jgrd.50712.

Kocurek, G., and N. Lancaster (1999), Aeolian system sediment state: Theory and Mojave Desert Kelso dune field example, *Sedimentology*, *46*, 505–515.

Lary, D. J., A. H. Alavi, A. H. Gandomi, and A. L. Walker (2016), Machine learning in geosciences and remote sensing, *Geosci. Front.*, *7*, 3–10, doi:10.1016/j.gsf.2015.07.003.

Lee, J. A., T. E. Gill, K. R. Mulligan, M. Dominguez Acosta, and A. E. Perez (2009), Land use/land cover and point sources of the 15 December 2003 dust storm in southwestern North America, *Geomorphology*, *105*, 18–27, doi:10.1016/j.geomorph.2007.12.016.

Lee, J. A., M. C. Baddock, M. J. Mbuh, and T. E. Gill (2012), Geomorphic and land cover characteristics of aeolian dust sources in West Texas and eastern New Mexico, USA, *Aeolian Res.*, *3*, 459–466.

Mahowald, N. M., et al. (2009), Atmospheric iron deposition: Global distribution, variability, and human perturbations, *Annu. Rev. Mar. Sci.*, *1*, 245–278, doi:10.1146/annurev.marine.010908.163727.

McTainsh, G. H., J. F. Leys, and W. G. Nickling (1999), Wind erodibility of arid lands in the Channel Country of western Queensland, Australia, *Z. Geomorphol.*, *116*, 113–130.

Novlan, D. J., M. Hardiman, and T. E. Gill (2007), *A Synoptic Climatology of Blowing Dust Events in El Paso, Texas From 1932–2005, Paper Presented at 16th Conference on Applied Climatology*, Am. Meteorol. Soc., San Antonio, Tex.

Parajuli, S. P., Z. L. Yang, and G. Kocurek (2014), Mapping erodibility in dust source regions based on geomorphology, meteorology, and remote sensing, *J. Geophys. Res. Earth Surf.*, *119*, 1977–1994, doi:10.1002/2014JF003095.

Prospero, J. M., P. Ginoux, O. Torres, S. E. Nicholson, and T. E. Gill (2002), Environmental characterization of global sources of atmospheric soil dust identified with the Nimbus 7 Total Ozone Mapping Spectrometer (TOMS) absorbing aerosol product, *Rev. Geophys.*, *40*(1), 1002, doi:10.1029/2000RG000095.

Reheis, M. C., and R. Kihl (1995), Dust deposition in southern Nevada and California, 1984–1989: Relations to climate, source area and source lithology, *J. Geophys. Res.*, *100*, 8893–8918, doi:10.1029/94JD03245.
Rivera Rivera, N. I., T. E. Gill, K. A. Gebhart, J. L. Hand, M. P. Bleiweiss, and R. M. Fitzgerald (2009), Wind modelling of Chihuahuan Desert dust outbreaks, *Atmos. Environ.*, *43*, 347–354.
Rivera Rivera, N. I., T. E. Gill, M. P. Bleiweiss, and J. L. Hand (2010), Source characteristics of hazardous Chihuahuan Desert dust outbreaks, *Atmos. Environ.*, *44*, 2457–2468, doi:10.1016/j.atmosenv.2010.03.019.
Sayer, A. M., N. C. Hsu, C. Bettenhausen, and M.-J. Jeong (2013), Validation and uncertainty estimates for MODIS Collection 6 "Deep Blue" aerosol data, *J. Geophys. Res. Atmos.*, *118*, 7864–7872, doi:10.1002/jgrd.50600.
Schepanski, K., I. Tegen, B. Laurent, B. Heinold, and A. Macke (2007), A new Saharan dust source activation frequency map derived from MSG-SEVIRI IR-channels, *Geophys. Res. Lett.*, *34*, L18803, doi:10.1029/2007GL030168.
Schmidt, R. H., Jr. (1979), A climatic delineation of the "real" Chihuahuan Desert, *J. Arid Environ.*, *2*, 243–250.
Schmidt, R. H., Jr. (1986), Chihuahuan Climate, in *Second Symposium on Resources of the Chihuahuan Desert Region U.S. and Mexico*, edited by J. C. Barlow, A. M. Powell, and B. N. Timmerman, pp. 40–63, Chihuahuan Desert Research Institute, Sul Ross State Univ., Alpine, Tex.
Scuderi, L. A., C. K. Laudadio, and P. J. Fawcett (2010), Monitoring playa lake inundation in the western United States: Modern analogues to late-Holocene lake level change, *Quaternary Res.*, *73*, 48–58.
Shao, Y., et al. (2011), Dust cycle: An emerging core theme in Earth system science, *Aeolian Res.*, *2*, 181–204, doi:10.1016/j.aeolia.2011.02.001.
Sweeney, M. R., E. V. McDonald, and V. Etyemezian (2011), Quantifying dust emissions from desert landforms, eastern Mojave Desert, USA, *Geomorphology*, *135*, 21–34, doi:10.1016/j.geomorph.2011.07.022.
Vickery, K. J., F. D. Eckardt, and R. G. Bryant (2013), A sub-basin scale dust plume source frequency inventory for southern Africa, 2005–2008, *Geophys. Res. Lett.*, *40*, 5274–5279, doi:10.1002/grl.50968.
Wang, X., D. Zia, T. Wang, X. Xue, and J. Li (2008), Dust sources in arid and semiarid China and southern Mongolia: Impacts of geomorphological setting and surface materials, *Geomorphology*, *97*, 583–600, doi:10.1016/j.geomorph.2007.09.006.
Washington, R., M. Todd, N. J. Middleton, and A. S. Goudie (2003), Dust-storm source areas determined by the Total Ozone Monitoring Spectrometer and surface observations, *Ann. Assoc. Am. Geogr.*, *93*, 297–313, doi:10.1111/1467-8306.9302003.
White, W. H., N. P. Hyslop, K. Trzepla, S. Yatkin, R. S. Rarig Jr., T. E. Gill, and L. Jin (2015), Regional transport of a chemically distinctive dust: Gypsum from White Sands, New Mexico (USA), *Aeolian Res.*, *16*, 1–10, doi:10.1016/j.aeolia.2014.10.001.
Woodage, M. J., and S. Woodward (2014), UK HiGEM: Impacts of desert dust radiative forcing in a high resolution atmospheric GCM, *J. Clim.*, *15*, 5907–5928, doi:10.1175/JCLI-D-13-00556.1.
Zender, C. S., D. J. Newman, and O. Torres (2003), Spatial heteorogeneity in aeolian erodibility: Uniform, topographic, geomorphic and hydrologic hypotheses, *J. Geophys. Res.*, *108*(D17), 4543, doi:10.1029/2002JD003039.